

Effect of quasi-monocrystalline porous silicon at the backside on the photovoltaic parameters of a polycrystalline silicon solar cell

A. Trabelsi, M. Krichen, A. Zouari and A. Ben Arab

Equipe de Modélisation des Composants Semi-Conducteurs, Laboratoire de Physique Appliquée,
Faculté des Sciences, Université de Sfax, B.P. 802, 3018, Sfax, Tunisie

(reçu le 23 Juin 2008 – accepté le 30 Septembre 2008)

Abstract - A three-dimensional model that simulates the performance of quasi-monocrystalline porous silicon (QMPS) at the backside reflector of an elementary polysilicon solar cell is developed. Analytical expression for the photocurrent generated under the effect of the reflected light is derived in the base region. An improvement effect is obtained on the photovoltaic parameters compared to conventional BSF polysilicon solar cell (without QMPS). The QMPS layer gives an improvement which overtakes 4 mA/cm^2 for the photocurrent, and 2.25 % for the cell efficiency. In addition, the effect of the QMPS layer is more important for a thin solar cell with passivated grain boundaries.

Résumé - Un modèle tridimensionnel est développé pour déterminer la performance d'une cellule solaire polycristalline avec du silicium poreux quasi-monocristallin (SPQM) en face arrière. La couche du SPQM est considérée comme un miroir pour la lumière permettant ainsi sa réflexion vers la cellule. Des expressions analytiques du photocourant généré par cette lumière réfléchiée dans la base sont obtenues. Une amélioration est obtenue dans les paramètres photovoltaïques comparés à ceux d'une cellule conventionnelle (sans SPQM). L'utilisation du SPQM en face arrière donne une amélioration qui dépasse 4 mA/cm^2 pour le photocourant, et 2.25 % pour le rendement de conversion. De plus, l'effet du SPQM est plus important pour une cellule solaire mince avec des joints de grains passivés.

Keywords: Polysilicon solar cells – Porous silicon – Rear surface – Light reflection.

1. INTRODUCTION

The potential of polycrystalline silicon for large scale terrestrial device application is well recognized. It shares with single-crystal silicon numerous desirable physical and chemical properties, while also showing great promise of reduced costs [1]. However, Defects are usually undesirable in polycrystalline silicon because they affect considerably the electrical properties of the semiconductor material by acting as charge carrier recombination/generation centres [2]. The presence of electric active grain boundaries in polycrystalline silicon is a serious limitation for the photovoltaic efficiency in comparison to monocrystalline silicon [3].

Many experimental studies that have employed the thin monocrystalline silicon cells, have used the porous silicon (PS) or quasi-monocrystalline porous silicon (QMPS) as a backside reflector for thin monosilicon solar cell to enhanced the effective thickness of crystalline silicon by the reflected light [4-6]. In addition, several simulations models for thin monosilicon solar cells with QMPS layer or PS on rear side have shown an improvement on the photocurrent as well as on the cell efficiency [4, 5].

It is expected that, for the same reason, the use of the QMPS on the back surface of a polysilicon solar cell may enhance the cell parameters. Considerable amount of experimental work has been reported on the polysilicon solar cell with QMPS on rear side, such as Nouri *et al.* [7] whose obtained an enhancement in the photocurrent density about $1\text{mA}/\text{cm}^2$ for a thick solar cell ($H = 400\ \mu\text{m}$).

The experimental study shows that the reflection due to the rear side for thin silicon solar cell is about 90% [8]. So this layer can be considered as a mirror for the light. Thus, the absorbed light in QMPS layer is very weak and the photocurrent generation in this region is neglected [8].

An analytical study is deemed necessary for determining the potential uses of this material as a backside layer in thin polysilicon solar cells. It is the purpose of this paper to present a simple analytical solution for the participation carried by this material (QMPS), to act as a backside reflector, on the cell photovoltaic parameters.

In this work, we consider an elementary $N^+/P/P^+$ polysilicon solar cell with a thin film QMPS on rear side. The increase in the photocurrent due to reflected light by QMPS layer is derived. The improvement on the photovoltaic parameters, namely photocurrent density J_{ph} and conversion efficiency η is discussed.

2. THEORY

We considered a polycrystalline $N^+/P/P^+$ solar cell with a thin film QMPS at the backside (Fig. 1). The grains boundaries are considered to be perpendicular to the surface of the cell with a depth that equal the grain thickness, and characterized by a recombination velocity V_g . The voids in the body of the QMPS layer are assumed to be spherical in size and uniformly distributed. The surface recombination velocities for the front and rear surfaces are S_p and S_n , respectively. The BSF is modelled by an effective surface recombination velocity in the vicinity of the low-high junction [9].

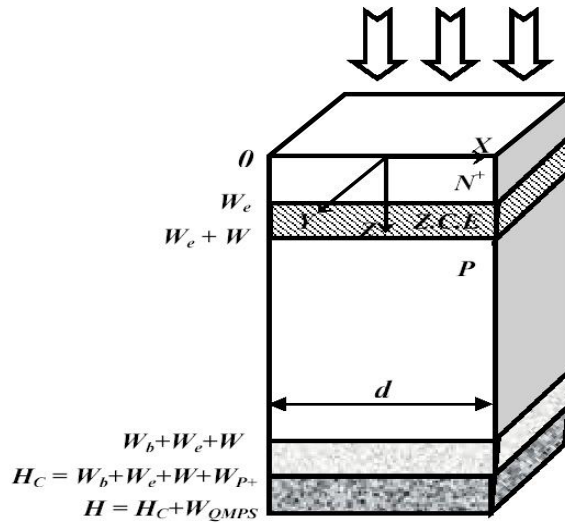


Fig. 1: Three-dimensional schematic model for an elementary solar cell with QMPS layer at the backside

The photocurrent density collectable from the solar cell at a wavelength in accordance with the earlier proposed model in reference [10] can be written as:

$$J_{\text{ph}}^{\text{T}}(\lambda) = J_{\text{ph}}^{\text{E}}(\lambda) + J_{\text{ph}}^{\text{B}}(\lambda) + J_{\text{ph}}^{\text{R}}(\lambda) + J_{\text{ph}}^{\text{ref}}(\lambda) = J_{\text{ph}}^{\text{C}}(\lambda) + J_{\text{ph}}^{\text{ref}}(\lambda) \quad (1)$$

$$\text{Where } J_{\text{ph}}^{\text{C}}(\lambda) = J_{\text{ph}}^{\text{E}}(\lambda) + J_{\text{ph}}^{\text{B}}(\lambda) + J_{\text{ph}}^{\text{R}}(\lambda) \quad (2)$$

$J_{\text{ph}}^{\text{C}}(\lambda)$ is the total photocurrent in a conventional BSF polysilicon solar cell without QMPS layer. And $J_{\text{ph}}^{\text{E}}(\lambda)$, $J_{\text{ph}}^{\text{B}}(\lambda)$ and $J_{\text{ph}}^{\text{R}}(\lambda)$ are the photocurrent densities that are collected from the emitter, the base and the depletion regions at N^+/P junction, respectively [11].

The contribution of the base region in the photocurrent density is obtained by solving analytically a three-dimensional continuity equation for the minority carrier given by [12]:

$$\frac{\partial^2 \Delta n(x,y,z,\lambda)}{\partial x^2} + \frac{\partial^2 \Delta n(x,y,z,\lambda)}{\partial y^2} + \frac{\partial^2 \Delta n(x,y,z,\lambda)}{\partial z^2} - \frac{\Delta n(x,y,z,\lambda)}{L_n^2} = \frac{g(z,\lambda)}{D_n} \quad (3)$$

Where Δn represents the concentration of excess minority carrier in the base (electrons); D_n and L_n are the diffusion constant and the diffusion length of minority electron in this region.

$g(z,\lambda)$ is the generation rate of minority carriers (electron) given by [12]:

$$g(z,\lambda) = (1 - R(\lambda)) \times \phi(\lambda) \times \alpha(\lambda) \times \exp(-\alpha(\lambda) \times z) \quad (4)$$

The reverse saturation current is obtained by solving the same continuity equation given by Eq. (1) but without the generation term [13].

Simple analytical expressions for the emitter photocurrent and reverse saturation current densities are taken from reference [14] using a one-dimensional model.

The photocurrent and the dark saturation current densities in the depletion region are taken from the reference [14].

We suppose that the additional component $J_{\text{ph}}^{\text{ref}}(\lambda)$ is contributed by the photo-generated carriers within the base region due to the reflected light.

Under illumination, the diffusion equation in the base for the reflected light may be written as:

$$\frac{\partial^2 \Delta n(x,y,z,\lambda)}{\partial x^2} + \frac{\partial^2 \Delta n(x,y,z,\lambda)}{\partial y^2} + \frac{\partial^2 \Delta n(x,y,z,\lambda)}{\partial z^2} - \frac{\Delta n(x,y,z,\lambda)}{L_n^2} = -\frac{g(z,\lambda)}{D_n} \quad (5)$$

The generation rate of minority carriers (electron) for the reflected light is given by [10]:

$$g_{\text{ref}}(z,\lambda) = (1 - R(\lambda)) \times R_d(\lambda) \times \phi(\lambda) \times \alpha(\lambda) \times \exp(-\alpha(\lambda)(2H - z)) \quad (6)$$

$R(\lambda)$ is the reflection coefficient through any reflecting layer at the front surface. We supposed also that the light reflectors are defined by the reflection coefficient noted $R_d(\lambda)$.

The boundary conditions used to solve the diffusion equation for this part of J_{ph}^B are [12]:

$$\Delta n(x, y, z = W_e + W) = 0 \quad (7)$$

$$\left. \frac{d\Delta n}{dz} \right|_{x=H} = -\frac{S_{e,P/P^+}}{D_n} \Delta n(x, y, z = H) \quad (8)$$

The expression of the reflected photocurrent density $J_{ph}^{ref}(\lambda)$ which is determined by solving the diffusion equation using the boundary conditions given by Eqs. (7) and (8) is as follows:

$$J_{ph}^{ref}(\lambda) = \frac{qD_n}{d^2} \int_{\frac{z}{d}}^{\frac{z}{d}} \int_{\frac{z}{d}}^{\frac{z}{d}} \left. \frac{\partial \Delta n}{\partial z} \right|_{z=W_e+W} dx dy \quad (9)$$

In our study, we have neglected the photo-generated carriers by the reflected light in the emitter region.

The photocurrent of the elementary solar cell with QMPS J_{ph}^T is given by:

$$J_{ph}^T = J_{ph}^C + J_{ph}^{ref} \quad (10)$$

Where J_{ph}^C is the total photocurrent in a conventional silicon solar cell without QMPS layer.

The increase of the photocurrent density due to the reflected light is given by:

$$\Delta J_{ph} = J_{ph}^T - J_{ph}^C = J_{ph}^{ref} \quad (11)$$

The conversion efficiency of an elementary cell with and without QMPS layer, are easily computed by :

$$\eta^T = \frac{V_m^T \times J_m^T}{P_{in}} \quad (12)$$

$$\eta^C = \frac{V_m^C \times J_m^C}{P_{in}} \quad (13)$$

The increase of the cell efficiency due to the reflected light is given by:

$$\Delta \eta = \eta^T - \eta^C \quad (14)$$

However, the maximum output power P_m of the cell can only be found by maximizing the power $P = V \times J(V)$ with respect to V . This gives rise to the well-known transcendental equation [15]:

$$\left(1 + \frac{V_m^i}{V_T}\right) \exp\left(\frac{V_m^i}{V_T}\right) = \frac{J_{ph}^i}{J_0^i} + 1 \quad \text{where } i = C \text{ or } T \quad (15)$$

And

$$J_m^i = J_0^i \exp\left\{\left(\frac{V_m^i}{V_T}\right) - 1\right\} + J_{ph}^i \quad \text{where } i = C \text{ or } T \quad (16)$$

V_m and J_m are the voltage and the current density at maximum power output.

3. RESULTS AND DISCUSSION

In this section, we discuss the results concerning the photocurrent density J_{ph} and the cell efficiency η of two types of polycrystalline silicon solar cells. The first solar cell is called conventional BSF solar cell (without QMPS layer) and in the second one, the rear side region is formed by a thin film QMPS.

The calculated variations concerning the different terms in photocurrent density (J_{ph}^C and J_{ph}^T) with respect to the grain width d are shown in Figure 2. It can be seen that the QMPS layer has an important effect on the photocurrent density especially for passivated grain boundaries. In this case, the enhancement in the photocurrent density is insensitive to the grain width and it overtakes 2 mA/cm^2 . However, for unpassivated grain boundaries, its effect is more remarkable for large grains. This result is confirmed by the Figure 3, which also shows that the influence of the cell thickness on the improvement of the photocurrent J_{ph}^{ref} due to the reflected light is more remarkable for the small grains.

The conversion efficiencies of a cell thickness with QMPS layer and of a conventional one, and the improvement in the efficiency due to the reflected light are calculated from Eqs. (12), (13) and (14) respectively and plotted against grain width as shown in figures 4 and 5.

The variation of efficiency with the grain width follows a trend similar to that of the photocurrent density. The solar cell with a QMPS layer and passivated grain boundaries has an efficiency about 16 % (Fig. 4). In addition, the enhancement of efficiency can overtake 2 % for a thin cell with passivated grain boundaries (Fig. 5).

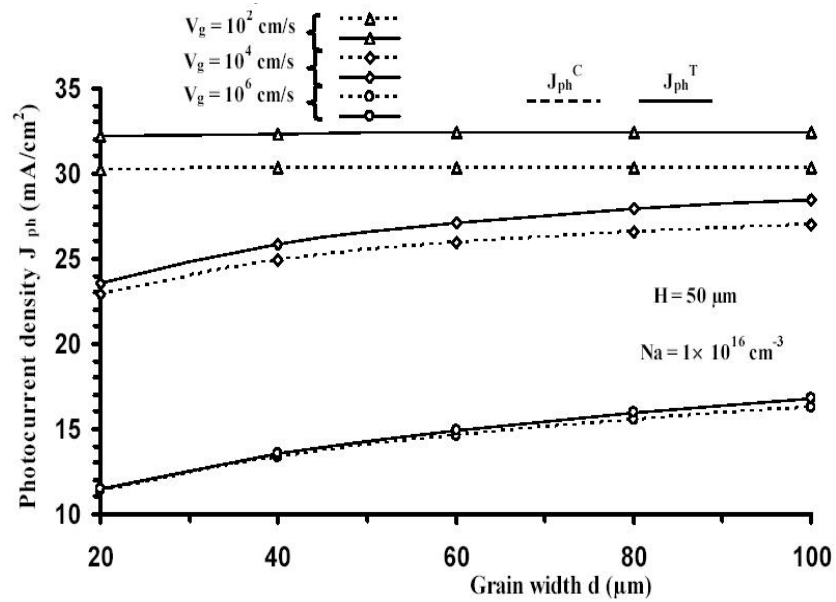


Fig. 2: Effect of the V_g on the variation of photocurrent density with respect to the grain width d for a cell with QMPS layer and for a conventional one

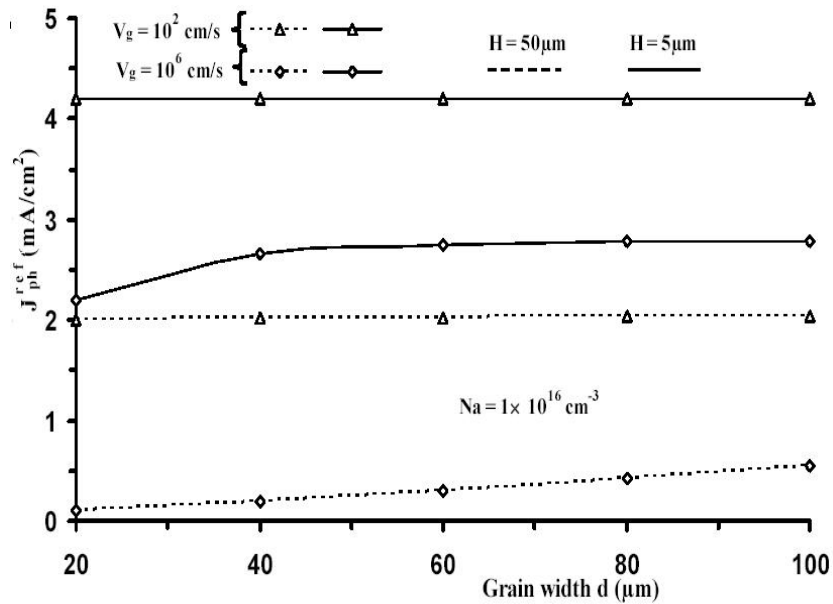


Fig. 3: Effect of the V_g on the variation of reflected photocurrent density with respect to the grain width d

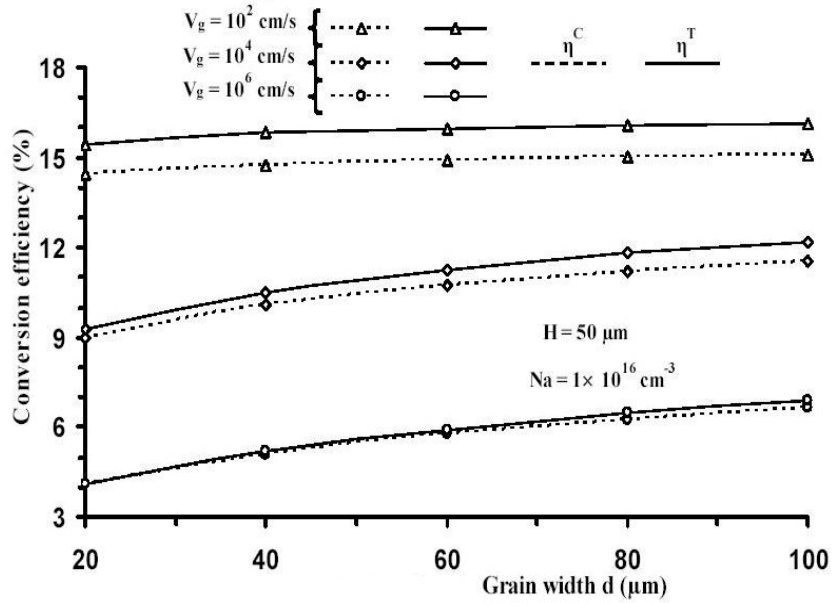


Fig. 4: Effect of the V_g on the variation of conversion efficiency with respect to the grain width d for a cell with QMPS layer and for a conventional one

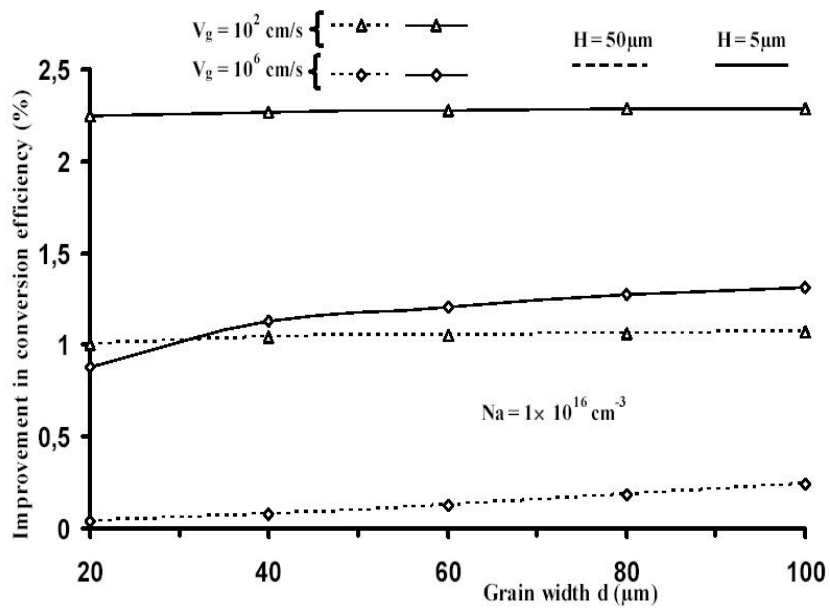


Fig. 5: Effect of the V_g on the variation of improvement in conversion efficiency with respect to the grain width d

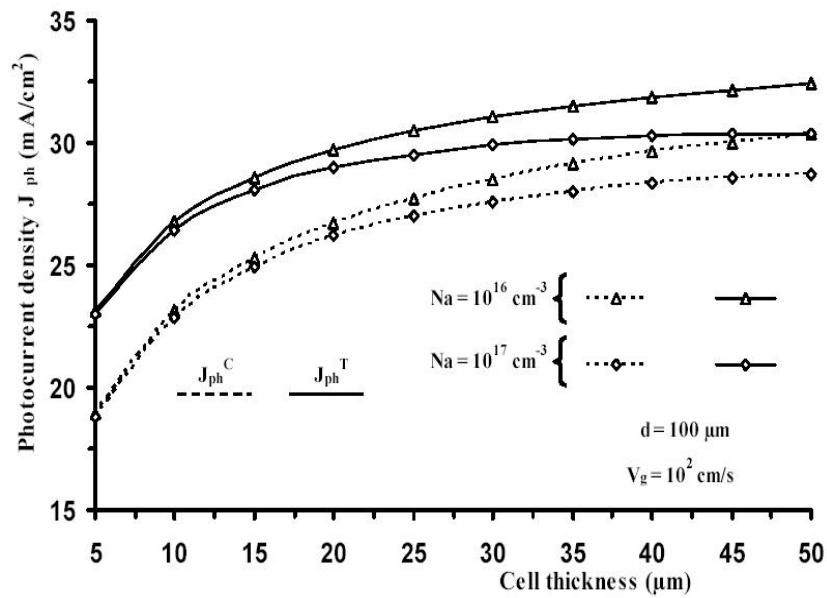


Fig. 6: Effect of the N_a on the variation of photocurrent density with respect To the cell thickness for a cell with QMPS layer and for a conventional one

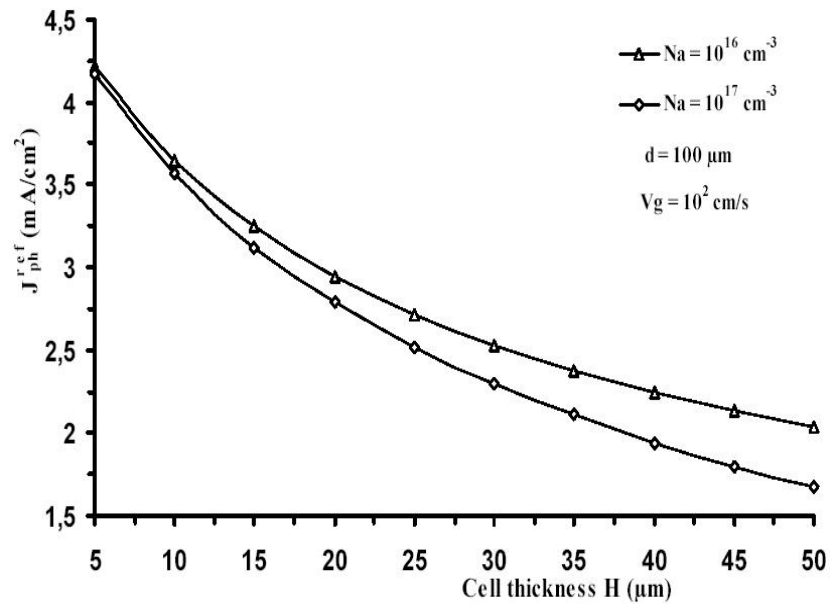


Fig. 7: Effect of the N_a on the variation of reflected photocurrent density with respect to the cell thickness

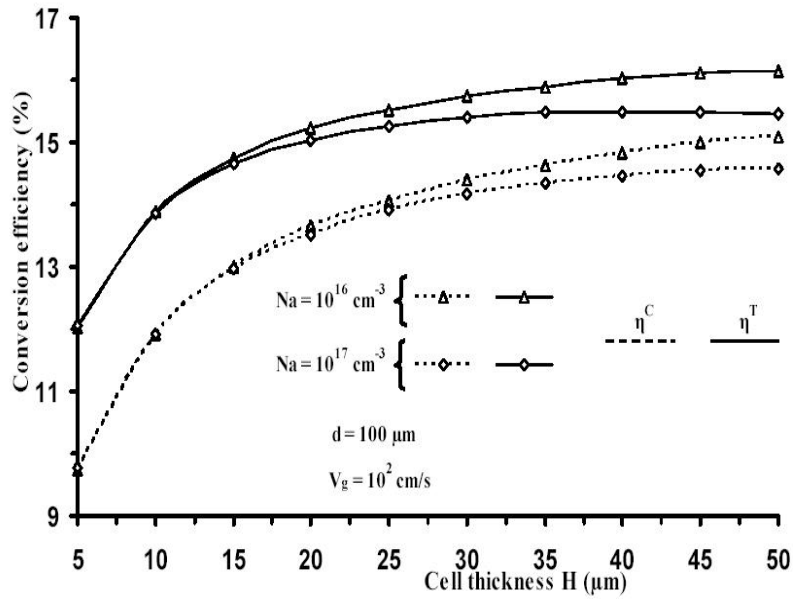


Fig. 8: Effect of the N_a on the variation of conversion efficiency with respect to the cell thickness for a cell with QMPS layer and a conventional one

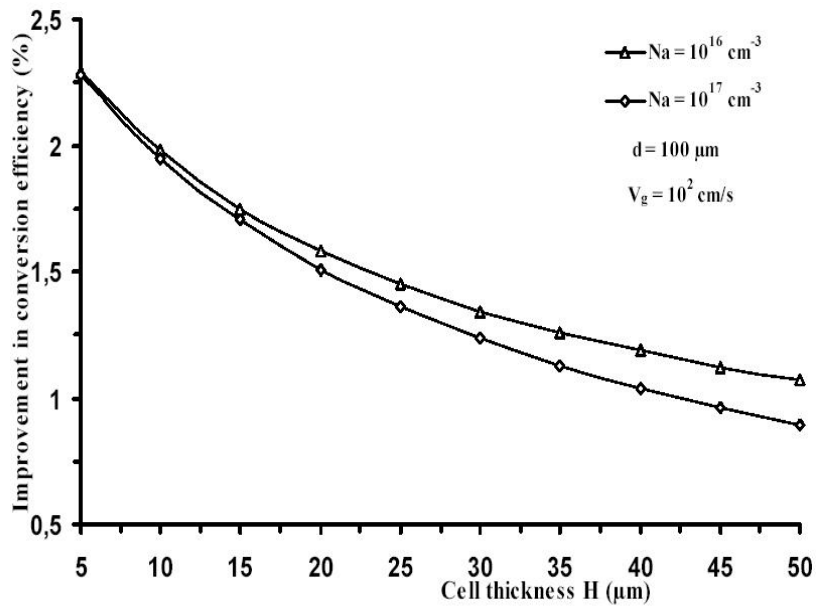


Fig. 9: Effect of the N_a on the variation of improvement in conversion efficiency with respect with respect to the cell thickness

In figure 6, we represent the effect of the cell thickness H (or H_c) on the photocurrent density for two values of the doping level in the base N_a . We noted that the QMPS layer has an important effect for a thin solar cell.

This results is due to the decrease of the generation rate of minority carriers for reflected lights $g_{ref}(z, \lambda)$ with respect to the cell thickness. In addition, the doping level in the base has practically no effect for a thin solar cell. The decrease of J_{ph}^{ref} is more remarkable for a high doping level in the base as it is indicated in figure 7.

Figures 8 and 9 show that the cell efficiency can overtakes 16 % and the enhancement due to the reflected light is about 2 % for a thick cell when the doping level is equal to 10^{16} cm^{-3} . Moreover, the variation of efficiency with the cell thickness follows a trend similar to that of the photocurrent density.

4. CONCLUSION

In this paper, an analytical model to simulate the performance of QMPS layer on rear side in an elementary polysilicon solar cell has been developed. A complete set of equations for the increases in the photocurrent due to the reflected light by a thin film QMPS have been solved analytically. It is seen that the photocurrent as well as the cell efficiency compared to conventional BSF thin silicon solar cell (without QMPS layer) has been improved. This improvement depends on the cell dimensions, the traps states at the grain boundaries and the doping level in the base. From the established results, the thin film QMPS rear surface contact solar cell show an enhancement which overtakes 4 mA/cm² in the photocurrent density and 2.25 % in the cell efficiency compared to conventional solar cells.

NOMENCLATURE

Q	Electron charge (C)
L_n	Diffusion length of minority carriers in the base region (cm)
D_n	Diffusion constants of minority carriers in the base region (cm ² .s ⁻¹)
τ_n	Minority carrier lifetime in the base region (s)
$N_a(N_a^+)$	Doping concentrations in the base (back) region (cm ⁻³)
$\alpha(\lambda)$	Absorption coefficient in the polysilicon at a wavelength (λ cm ⁻¹)
$\phi(\lambda)$	Incident photon flux (cm ⁻² .s ⁻¹)
W_b W_b	Base thickness (cm)
$H(H_c)$	Total cell thickness with (without) QMPS layer (cm)
$S_p(S_n)$	Recombination velocity at the front (back) contact (cm.s ⁻¹)
ΔJ_{ph}	Increase in photocurrent density by QMPS layer (mA.cm ⁻²)

$\Delta \eta$	Increase in cell efficiency by QMPS layer (%)
P_{in}	Output power density (AM 1.5) ($mW.cm^2$)
P_m	Maximum output power of solar cell (mW)

REFERENCES

- [1] S.N. Mohammad and C.E.Rogers, Solid-State Electronics, Vol. 31, pp. 1221 - 1228, 1988.
- [2] J. Dugas, Solar Energy Materials and Solar Cells, Vol. 43, pp. 193 - 202, 1996.
- [3] A. Rohatgi and P. Rai-Choudhury, IEEE Transactions on Electron Device, Vol. 31, N°5, 1984.
- [4] R. Brendel, Solar Energy, Vol. 77, pp. 969 - 982, 2004.
- [5] R.B. Bergmann, C. Berge, T.J. Rinke, J. Schmidt and J.H. Werner, Solar Energy Materials and Solar Cells, Vol. 74, pp. 213 - 218, 2002.
- [6] R. Bilyalov, C.S. Solanki, J. Poortmans, O. Richard, H. Bender, M. Kummer and H. von Känel, Thin Solid Films, Vol. 403-404, pp. 170 - 174, 2002.
- [7] H. Nouri, W. Dimassi, M. Bouaicha, M.Hajji, M.F. Boujmil, M. Saâdoun, B. Bessaïs, H. Ezzaouia and R. Bennaceur, Thin Solid films, Vol. 451-452, pp. 312 - 315, 2004.
- [8] M. Banerjee, S.K. Dutta, U. Gangopadhyay, D. Majumdar and H. Saha, Solid-State Electronics, Vol. 49, pp. 1282 - 1291, 2005.
- [9] A. Rohatgi and P.R. Choudhury, IEEE Transactions on Electron Devices, Vol. 31, p 596, 1984.
- [10] S.K. Mehta and S.C. Jain, Solar Cells, Vol. 8, pp. 337 - 353, 1983.
- [11] S.M. Sze, Physics of Semiconductors Devices, Bell Laboratories Inc., New-Jersey, 1991.
- [12] A. Ben Arab, Solid-States Electronics Vol. 37, p. 1395, 1994.
- [13] M. Ben Amar, Rev. Int. d'Héliotechnique, Vol. 3, p. 24, 2001.
- [14] A. Ben Arab, Solar Cells, Vol. 29, p. 49, 1991.
- [15] A. DE Vos, Solar Cells, Vol. 8, pp. 283 - 296, 1983.